Published in final edited form as:
Biomaterials. 2009 October ; 30(29): 5283–5291. doi:10.1016/j.biomaterials.2009.06.032.

Factors affecting size and swelling of poly(ethylene glycol) microspheres formed in aqueous sodium sulfate solutions without surfactants

Michael D. Nichols, **Evan A. Scott**, and **Donald L. Elbert***
Department of Biomedical Engineering and Center for Materials Innovation, Washington University in St. Louis, Campus Box 1097, One Brookings Dr., St. Louis, MO 63130

Abstract

The LCST behavior of poly(ethylene glycol) (PEG) in aqueous sodium sulfate solutions was exploited to fabricate microspheres without the use of other monomers, polymers, surfactants or organic solvents. Reactive PEG derivatives underwent thermally induced phase separation to produce spherical PEG-rich domains that coarsened in size pending gelation, resulting in stable hydrogel microspheres between ≈1–100 microns in size. The time required to reach the gel point during the coarsening process and the extent of crosslinking after gelation both affected the final microsphere size and swelling ratio. The gel point could be varied by pre-reaction of the PEG derivatives below the cloud point, or by controlling pH and temperature above the cloud point. Pre-reaction brought the PEG derivatives closer to the gel point prior to phase separation, while the pH and temperature influenced the rate of reaction. Dynamic light scattering indicated a percolation-to-cluster transition about 3–5 minutes following phase separation. The mean radius of PEG-rich droplets subsequently increased with time to the $1/4^{th}$ power until gelation. PEG microspheres produced by these methods with controlled sizes and densities may be useful for the production of modular scaffolds for tissue engineering.

Keywords

poly(ethylene glycol); microsphere; LCST; hydrogel; scaffold; cloud point; thermally induced phase separation

Introduction

Hydrogel microparticles are useful in a wide variety of applications spanning from chromatography resins to surface coatings [1,2]. A new and promising application of hydrogel microparticles is their use as building blocks for the assembly of modular scaffolds [3–5]. A variety of methods are available to produce hydrogel microspheres for modular scaffolds. Mechanical methods include micromolding, atomization or microfluidics, which allow precise control over size but produce microspheres in a serial manner [5–7]. Solution-phase methods such as precipitation/dispersion or emulsion polymerization are highly scalable but often require the use of organic solvents, surfactants or other additives that may negatively impact biocompatibility [8]. Precipitation/dispersion polymerization of PEG-acrylate and N-

*To whom correspondence should be addressed: Donald L. Elbert, Campus Box 1097, One Brookings Dr., St. Louis, MO 63130, Tel: (314) 935-7519, Fax: (314) 935-7448, elbert@biomed.wustl.edu.

Competing Financial Interests
The authors have no competing financial interests.

isopropylacrylamide in water at 70°C produces sub-micron microgels that are about 60% PEG by mass [2]. Emulsion polymerization of phase-separated PEG/dextran in water also results in microsphere formation [9–11]. Due to the ability of PEG to resist non-specific protein adsoption [12], it may be desirable to produce PEG microspheres by a solution-phase method that does not rely on organic solvents, surfactants or other additives, as these may be difficult to remove later. Hennink and colleagues previously used an emulsion polymerization to produce PEG microspheres in aqueous magnesium sulfate solutions. The two phase solutions were vigorously mixed but large aggregates of microspheres formed when crosslinked following a thermally-induced phase separation [9].

PEG phase separates above a lower critical solution temperature (LCST) that can be lowered to less than room temperature in the presence of kosmotropic salts [13–15]. Phase separation occurs by nucleation and growth or by spinodal decomposition, dependent upon if the spinodal line is crossed. The binodal and spinodal lines are affected by the molecular weight of the PEG, such that no single LCST may be associated with a PEG solution undergoing crosslinking. Furthermore, away from the critical concentration, single phase solutions exist between the LCST and the binodal line. For simplicity, a cloud point temperature corresponding to the binodal line is often reported rather than an LCST [14]. Following phase separation by nucleation or spinodal decomposition, phase-separated domains grow in size (coarsen) by coalescence and/or Ostwald ripening [16,17]. Coalescence results from collision and subsequent fusion of minority phase-separated domains caused by Brownian motion, fluid flow or buoyancy effects [18]. Ostwald ripening results from mass transfer from smaller domains to larger domains by diffusion of minority phase molecules through the majority phase [19]. In both coalescence and Ostwald ripening, the mean sizes of the phase-separated domains evolve as $\bar{r} \propto time^{1/3}$, where $\bar{r}$ is a characteristic length scale of the phase-separated domains [18–20]. Given enough time, coarsening results in the formation of two distinct phase separated layers due to differences in the densities of the phases.

We demonstrate here that 100% PEG microspheres may be formed in unstirred aqueous salt solutions. To form microspheres, reactive PEG derivatives were mixed and gelled soon after a thermally induced phase separation. The sizes of the formed microspheres were affected by the rate of reaction relative to the rate of coarsening and the extent of reaction both before and after phase separation. The fabrication method is simple, reproducible, scalable and does not rely on the use of organic solvents, surfactants, co-monomers or other additives.

2. Materials and Methods

2.1. Pre-reaction of PEG derivatives below the cloud point

Unless otherwise noted, all reagents were purchased from Sigma-Aldrich. Eight-arm PEG-OH (PEG_8-OH; mol. wt. 10,000; Shearwater Polymers, Huntsville, AL) was used to synthesize PEG_8-vinylsulfone (PEG_8-VS), PEG_8-acrylate and PEG_8-amine, which were synthesized as previously described [21,22]. PEG_8-VS and PEG_8-amine solutions were prepared at 20% (w/v) in Dulbecco's phosphate buffered saline (Pierce) and sterile filtered with 0.22 μm syringe filters (Millipore). PEG_8-VS was 'pre-reacted' with PEG_8-amine below the cloud point by combining the solutions at a 1:1 ratio of vinylsulfone to amine groups for a total volume of 1 mL in 1.5 mL centrifuge tubes. Once mixed, these solutions were reacted by incubation at 37°C with rotation at 40 rpm. The progress of the reactions was followed by dynamic light scattering (DLS) until the desired mean effective diameter (d_{PCS}) was reached. For gel permeation chromatography, PEG_8-VS was reacted with PEG_8-amine to a $d_{PCS} \cong 50$ nm. The reaction was stopped by incubation with 2-mercaptoethanol for 1 h at 37°C at a thiol:vinylsulfone ratio of 2:1, which did not change the d_{PCS}. GPC was performed by PolyAnalytik (London, ON, Canada) using a Viscotek Model 302-050 detector detecting light scattering, viscosity and refractive index. Samples (0.5 mg PEG) were dissolved in 0.05 M

sodium nitrate. Three columns were used in series (PolyAnalytik High Resolution Aqueous Columns: PAA-202.5, exclusion limit 10 kDa; PAA-203, exclusion limit 100 kDa; PAA-206M, exclusion limit 20 MDa) calibrated with poly(ethylene oxide) standards.

2.2. Cloud point determination

Solutions of PEG_8-VS, PEG_8-acrylate or PEG_8-amine were diluted to 2% (w/v) from the 20% (w/v) stock solutions with PBS and PBS + 1.5 M sodium sulfate to achieve the desired sodium sulfate concentration. Cloud points of the polymers were determined by increasing solution temperatures in a thermal cycler in 2°C steps (PCR Sprint Thermal Cycler, Thermo Electron Corp.) and visually observing the temperature at which the cloud point was reached.

2.3 Fluorescent labeling of PEG derivatives

A 20% (w/v) solution of PEG_8-VS in PBS was incubated with L-cysteine in a 100:1 ratio of PEG:cysteine at 37°C for 30 min. A 10 mg/mL solution of Dylight-488 NHS-ester (Pierce) in dimethylformamide was then added to the solution in a 1:1 ratio of cysteine:Dylight-488 and incubated overnight at 25°C to produce fluorescent PEG_8-VS. To fluorescently label PEG_8-amine, a 10 mg/mL solution of Dylight-488 or Dylight-633 (Pierce) in dimethylformamide was added to a 20% (w/v) solution of PEG_8-amine in a 100:1 ratio of PEG:dye and incubated overnight at 25°C.

2.4. Microsphere fabrication and characterization

PEG_8-VS/PEG_8-amine microspheres were fabricated from pre-reacted solutions of PEG_8-VS and PEG_8-amine ($d_{PCS} \cong 100$ unless otherwise stated). The 20% (w/v) PEG pre-reacted solutions were diluted to 2% (w/v) PEG with PBS and PBS + 1.5 M sodium sulfate to a final sodium sulfate concentration of 0.6 M and volume of 50 μL. The PEG_8-VS/PEG_8-amine solutions were then incubated above the cloud point at 37°C for 45 min unless otherwise stated. Suspensions of microspheres were subsequently buffer exchanged into PBS 2× to remove the sodium sulfate by: (1) diluting the microsphere solution 3:1 with PBS and titurating, (2) centrifuging at 14,100*g* for 2 min, (3) removing the supernatant. Phase contrast photomicrographs of microspheres at 20× were used to analyze the sizes of >500 microspheres at each condition from three separately prepared samples. Microspheres were manually thresholded and quantified with ImageJ software (NIH). Comparisons were made by one-factor ANOVA with a Scheffe *post-hoc* test. PEG_8-acrylate/PEG_8-amine microspheres were produced as above but in PBS + 0.8 M sodium sulfate incubated 5 min at room temperature and then 5 min at 95°C.

2.5. Dynamic light scattering (DLS)

Mean effective hydrodynamic diameters (d_{PCS}) of pre-reacted solutions were monitored by dynamic light scattering/photon correlation spectroscopy (DLS/PCS; 90Plus Particle Size Analyzer, Brookhaven Instruments, Holtsville, NY) at a scattering angle of 90° and wavelength of 658 nm. Calculation of d_{PCS} and statistical analysis of the results were performed using Brookhaven Instruments Particle Sizing Software (version 2.34, Brookhaven Instruments). Disposable polystyrene cuvettes (Brookhaven Instruments) were cleaned 1× with 95% ethanol and 2× with DI water prior to use. The progression of oligomer/microgel growth was monitored by diluting samples (30 μL) with PBS (3 mL final volume) prior to analysis at 25°C. Coarsening of PEG-rich phases was also monitored by DLS (3 mL, 1 or 2% (w/v) PEG, PBS + 0.6 M sodium sulfate). Mean effective diameters of the phase-separated domains were measured as the temperature of the solutions was raised to 37°C within the instrument.

2.6. Confocal microscopy

Fluorescence microscopy was performed with a Nikon Eclipse C1/80i confocal microscope. Suspensions of fluorescently labeled derivatives or microspheres were imaged on glass microscope slides (Corning Inc.) with a 20× objective (0.45 DIC L WD 7.4). Images were processed using EZ-C1 3.70 FreeViewer software (Nikon Instruments Inc.).

2.7. Statistics

A p-value < 0.05 was considered significant. Data were mean ± standard deviation unless otherwise indicated.

3. Results

3.1. Microsphere fabrication

Hydrogel microspheres were formed by crosslinking PEG macromonomers above the cloud point (Fig. 1). Initial reaction of the PEG macromonomers below the cloud point ('pre-reaction') was found to influence the reaction time required to obtain stable microspheres. Below the cloud point, reaction of eight-arm PEG-vinylsulfone (PEG_8-VS, 10 kDa) with eight-arm PEG-amine (PEG_8-amine, 10 kDa) in a 1:1 molar ratio at a concentration of 20% (w/v) PEG in phosphate buffered saline (PBS, pH 7.4) resulted in the formation of a bulk hydrogel in about 7 h at 37°C. The progress of the pre-reaction toward the gel point was followed by dynamic light scattering/photon correlation spectroscopy (DLS/PCS), which provided an intensity-weighted (i.e. z-average) measure of the mean effective diameter (d_{PCS}) of polymers in the reacting solution. A d_{PCS} of about 10 nm was observed after a few hours of reaction while a d_{PCS} of about 180 nm was found just prior to gelation. Solutions reacted to a $d_{PCS} \cong$ 50 nm were characterized by gel permeation chromatography (GPC), which revealed that PEG microgels with >10 nm hydrodynamic radius constituted 32.6 wt% of the PEG (Fig 2A). Monomeric (i.e. unreacted) PEG comprised 12.9 wt% of the PEG, with the remainder of solution being oligomers of PEG_8-VS and PEG_8-amine. The intensity-weighted signal of right angle light scattering was much more sensitive to the presence of larger reacted PEG species (microgels) than monomers and oligomers, as expected (Fig. 2B). Thus, the d_{PCS} from DLS was a measure of the average size of only the largest PEG oligomers/microgels, but was a useful metric to monitor the progress of pre-reaction. Solutions pre-reacted to $d_{PCS} \cong$ 100 nm were diluted to 2% (w/v) PEG in PBS + 0.6 M sodium sulfate at room temperature. Dilution was important to slow the rate of the pre-reaction, as a solution with $d_{PCS} \cong$ 100 nm was about 30 min from the gel point at 20% (w/v) PEG and 37°C. Diluted to 2% (w/v), gelation was not observed within 24 h, consistent with a 100-fold decrease in the rate of the second order reaction expected for the 10-fold dilution. The solutions were diluted in PBS + 0.6 M sodium sulfate, which was below the cloud point of the solution at room temperature. To cause phase separation, the temperature of the diluted solution was raised to 37°C, producing spherical, PEG-rich domains. Within 45 min, stable PEG_8-VS/PEG_8-amine microspheres formed that were stable following buffer exchange into PBS (Fig. 3A). As the length of the pre-reaction step was increased, i.e. at larger d_{PCS} values, the sizes of the formed microspheres decreased (Fig. 3B). Generally, microspheres formed aggregates during production that were easily dispersed via tituration.

The importance of pre-reacting the components before phase separation may have been due to the dramatic difference in the cloud point between PEG_8-VS and PEG_8-amine. The cloud point of 2% (w/v) PEG_8-VS in PBS + 0.6 M sodium sulfate was close to room temperature, while the cloud point of the cationic PEG_8-amine was >100°C (Fig. 4A). Eight-arm PEG-acrylate (PEG_8-acrylate, 10 kDa) was found to phase separate at lower temperatures than PEG_8-VS. DLS was used to investigate the effects of the charged PEG_8-amine on the early stages of coarsening above the cloud point of PEG_8-VS (Fig. 4B). A linear relationship was found

between the mean diameter of the phase-separated domains and time, which is expected in the early stages of phase separation [23]. A plateau in coarsening was reached 3–5 minutes after phase separation that may correspond to a percolation-to-cluster transition [23]. Following a percolation-to-cluster transition, growth is expected to slow from $\bar{r} \propto time$ to $\bar{r} \propto time^{1/4}$ or $\bar{r} \propto time^{1/3}$, where $\bar{r}$ is the mean radius [20,23,24]. The rate of coarsening of a PEG_8-VS solution was not greatly affected by the presence of PEG_8-amine if the two components were mixed just prior to raising the temperature above the cloud point. However, pre-reaction of PEG_8-VS with PEG_8-amine to a $d_{PCS} \cong 100$ nm led to a delay in phase separation and a plateau at 700 nm instead of 1400 nm, indicating that PEG_8-amine may have had a stabilizing or emulsifying effect on the phase-separated PEG.

3.2. Confocal microscopy of microspheres during formation

Coarsening was further investigated by visualizing fluorescently labeled, phase-separated PEG derivatives via confocal microscopy. To observe Ostwald ripening, solutions of fluorescent PEG_8-VS and fluorescent PEG_8-amine were separately raised above their cloud points in PBS + 1.2 M sodium sulfate and then mixed (Fig. 5A&B). Without detecting coalescence, the fluorescent PEG derivatives transferred between the two types of spherical domains over time. The exchange must have occurred via mass transfer through the majority phase, indicating that Ostwald ripening may contribute to the coarsening of the PEG domains. Coarsening was also visualized by confocal microscopy using a salt concentration more typical for microsphere formation (PBS + 0.6 M sodium sulfate). Fluorescent PEG_8-VS and fluorescent PEG_8-amine were pre-reacted to a $d_{PCS} \cong 100$ nm and then heated for 15 min at 37°C. The ratio of PEG_8-VS to PEG_8-amine within the spherical domains varied between microspheres, as judged by the relative fluorescence intensities. Some of these spherical domains were observed to coalesce, forming larger spheres with an intermediate ratio of the two types of PEG (Fig. 5C).

Over the course of 20 min, coalescence of PEG-rich domains became less frequent and unlabeled regions began to appear. Both PEG derivatives were fluorescently labeled and thus the unlabeled region was a water-rich, polymer-poor phase (Fig. 6A). Water-rich domains grew in size within the PEG-rich spherical domains. Eventually, the water-rich droplets ceased to grow in size suggesting that the PEG-rich domains had reached the gel point. To better visualize the structure of the formed microspheres, relatively large fluorescent microspheres (≈100 μm instead of ≈10 μm) were generated by lowering the cloud point to below room temperature and allowing the solution to coarsen at room temperature for 5 min before raising the temperature to 37°C for 45 min. The stable, buffer exchanged microspheres were found to be porous, with a wide range of pore sizes (Fig. 6B(i)). Microspheres were also produced using a similar methodology from pre-reacted solutions of PEG_8-acrylate and PEG_8-amine, which exhibited the same porous structure (Fig. 6B(ii)).

3.3. Effects of length of reaction above the cloud point, pH and temperature on microsphere size

During buffer exchange into PBS to remove sodium sulfate, microspheres swelled to much greater sizes (Fig. 7). The swelling ratio (Q, the increase in volume after buffer exchange) decreased with increasing reaction time above the cloud point (Table 1). Increasing lengths of reaction above the cloud point resulted in decreasing swollen microsphere sizes, but after 45 min at pH 7.4 or 75 min at pH 6.5, the swollen microsphere sizes did not decrease further (Fig. 8A). Despite the large differences in the sizes of microspheres following buffer exchange into PBS (‘swollen’), the sizes of the microspheres prior to buffer exchange (‘unswollen’) were unaffected by the length of time above the cloud point. A lower pH during the crosslinking reaction increased the sizes of both swollen and unswollen microspheres, which is contrasted with the length of reaction time that only affected the sizes of swollen microspheres (Table 1; Fig. 8B). The swelling ratio was not greatly affected by the pH of the reacting solution (Table

1). Temperature was also observed to impact microsphere size, with higher reaction temperatures resulting in smaller microspheres (Fig. 9). The polydispersity index of microspheres was measured as a function of pH and was 3.3 for microspheres formed at pH 7.4 (Fig. 8B, inset). The observed distributions of the microspheres more closely resembled that expected for coalescence than for Ostwald ripening (Fig. 10).

4. Discussion

Several factors influenced the production of 100% PEG microspheres via thermally induced phase separation in the absence of surfactants or organic solvents. Microsphere sizes were affected by the extent of pre-reaction below the cloud point, pH, temperature, and the duration of the crosslinking reaction above the cloud point. The results suggested that the final swollen microsphere sizes were determined primarily by two factors: the degree of coarsening of PEG-rich domains prior to reaching the gel point and the extent of crosslinking within microspheres beyond the gel point.

Coarsening of the phase-separated PEG-rich domains occurred by a combination of Ostwald ripening and coalescence. Although the two mechanisms follow the same growth law, $\bar{r} \propto time^{1/3}$, they can be distinguished by the resulting microsphere size distributions [20]. During coarsening, the sizes of phase-separated domains are polydisperse and the observed microsphere size distributions likely reflected the polydispersity of the phase-separated domains at the time of gelation [18–20,25]. The PEG microsphere size distributions displayed a leftward-shifted mean, indicative of coarsening dominated by coalescence instead of Ostwald ripening (Fig. 10) [20]. This conclusion was further validated by the frequent observation of coalescence by confocal microscopy under conditions typical for microsphere formation (Fig. 5).

Coarsening was halted by gelation and thus the length of time required to reach the gel point was a major determinant of microsphere sizes. The rate of reaction should increase with increasing temperatures according to the Arrhenius equation, and thus the gel point will be reached earlier. With less time for coarsening, smaller sized microspheres would be expected, agreeing with our observation (Fig. 9). In principle, coarsening should also proceed more quickly at high temperatures leading to larger microspheres, but apparently temperature affected the reaction rate more than the coarsening rate.

Increased pre-reaction below the cloud point resulted in the formation of smaller microspheres. Pre-reaction of the PEG-derivatives should simply bring the solution closer to the gel point. With less time required for gelation, the gel point would occur earlier in coarsening, resulting in smaller microspheres. The effect of pre-reaction on microsphere size was analyzed via a power law plot of the data in Figure 3B. The pre-reaction times were expressed as the fraction of time remaining to reach the gel point, $(t_{gel} - t_{pre\text{-}reaction})/t_{gel}$. The gel point ($t_{gel}$) was reached in 7 h under the standard conditions (pH 7.4, 20% (w/v) PEG, 37°C). The power law plot of microsphere mean diameters versus the fractional time remaining to reach the gel point led to a reasonable linearization of the data, with a slope of 0.24 (Figure 11A). This suggested a $\bar{r} \propto time^{1/4}$ growth law.

Similarly, pH influenced microsphere size, with lower pH resulting in larger microspheres. The rate of the reaction between the vinylsulfone and amine is decreased at low pH due to a decrease in the concentration of highly nucleophilic unprotonated amines. The observed rate constant as a function of pH for the second order reaction is $k_{obs} = k_2/(1+10^{pKa-pH})$, where k_2 is the rate constant for reaction of vinylsulfone with the unprotonated amine [26]. The effect of pH was analyzed by assuming that the mean time to reach the gel point was the major determinant of microsphere size. The mean time to reach the gel point for this second-order

reaction should scale with pH as $time \propto 1 + 10^{pKa-pH}$ (see Supplemental Materials for further discussion). Thus, a plot of log(mean microsphere diameter) versus $\log(1 + 10^{pKa-pH})$ should yield a straight line with a slope of 1/3 if the $\bar{r} \propto time^{1/3}$ growth law is followed. Linear regression supported such a power law relationship, but with a measured slope of 0.24, which is the same slope observed for the power law plot of mean microsphere diameters versus fractional time remaining for gelation. Microspheres formed at pH 6 and 6.5 were not included in the analysis because their swollen sizes were far from asymptotic at 45 min as judged by the results in Figure 8A and thus should swell to much greater extents than microspheres produced at higher pHs.

Both power law plots supported an $\bar{r} \propto time^{1/4}$ growth law instead of a growth law, which is plausible based on previous results in the literature. Immediately following phase separation, the PEG-rich domains may be connected in a percolated, network-like structure [27]. Surface tension drives the flow from the thin, connected web of phase separated polymer into larger clusters [28]. During this initial flow-driven period, a relatively rapid $\bar{r} \propto time$ growth law is followed [23,27]. Upon reaching the percolation-to-cluster transition, the growth law changes to $\bar{r} \propto time^{1/4}$, eventually evolving to the classical $\bar{r} \propto time^{1/3}$ growth law [23,24]. Analysis of the early stages of phase separation by DLS (Figure 4B) supported the $\bar{r} \propto time$ growth law immediately following phase separation. Power law plots of d_{PCS} versus time for the DLS results revealed exponents in the range of 0.67, 1.0, 0.84 and 1.7 for 1% PEG, 2% PEG, PEG_8-VS/PEG_8-amine without pre-reaction, and PEG_8-VS/PEG_8-amine with pre-reaction, respectively. After about 4 min, DLS indicated a plateau or asymptote in domain size growth. These findings are consistent with light scattering studies of polymer solutions following thermally induced phase separation, in which an initially linear growth regime was followed by a period of much slower growth [27]. Molecular dynamics simulations suggest a transition from the $\bar{r} \propto time$ growth law to a $\bar{r} \propto time^{1/4}$ growth law [24]. The $\bar{r} \propto time^{1/4}$ growth law observed here may reflect that the gel point is reached during this intermediate period of phase separation. However, we cannot dismiss the potential effects of the loss of small microspheres during washing or the inability to observe small microspheres by phase contrast microscopy at 20× magnification. Smaller microspheres would more likely be excluded from the mean values of the faster gelling conditions. This may skew the slope of the power law plots downward due to overestimating the average size of microspheres for the fastest gelling conditions. Nonetheless, the similar exponents obtained in two separate sets of experiments suggest that the $\bar{r} \propto time^{1/4}$ growth law governs the sizes of microspheres formed under these conditions.

The length of incubation time above the cloud point also influenced the sizes of microspheres that formed, but the mechanism was not directly related to the gelation time. While the pH affected the sizes of both swollen (i.e. buffer exchanged) microspheres and unswollen microspheres (i.e. still above the cloud point), the length of incubation beyond the gel point only affected the sizes of the swollen microspheres (Table 1). Coarsening should be halted after the PEG-rich domains reached the gel point and further reaction should not alter the sizes of unswollen microspheres. Further reaction beyond the gel point should only increase the density of crosslinks within the microspheres, affecting the degree of swelling following buffer exchange. The expected relationship between swelling and crosslink density $Q \propto M_c^{3/5}$ is according to the Flory-Rehner equation, where Q is the swelling ratio and M_c is the molecular weight between crosslinks [29]. The molecular weight between crosslinks will decrease as the reaction proceeds and will be determined by the rate of the second order reaction between vinylsulfone and amine groups and the combinatorics of the end-group reaction. However, quantitative analysis is not possible without detailed knowledge of the kinetics of the crosslinking reaction and the nature of defects in the network structure. Qualitatively, the decrease in mean diameter found with increasing reaction time was consistent with the expected decrease in Q with decreasing M_c.

The current method produced microspheres that were not only polydisperse but were also porous. Pore formation has been previously observed in gelatin coacervates, in which vacuoles developed following a decrease in temperature [30]. In PEG/water biphasic systems, an increase in molecular weight broadens the binodal curve, increasing the PEG equilibrium concentration in the PEG-rich domains [14]. Thus, water should be released during crosslinking to form water-rich domains inside the PEG-rich domain. These water-rich domains coarsen inside the PEG-rich phase, resulting in pores after gelation if the water-rich domains are unable to diffuse to the surface of the PEG-rich phase. Additionally, clusters of microspheres developed over time in solution and likely resulted from the reaction of residual vinylsulfone and amine groups present within the microspheres. Occasionally, microspheres were observed that appeared to consist of two or more microspheres that gelled while coalescing. The polydispersity in microsphere sizes, porosity, and slight aggregation produced by this method are inherent in the formation mechanism and must be compatible with the end application of the microspheres.

5. Conclusion

The two major factors that determined microsphere sizes were the extent of coarsening that occurred prior to gelation and the extent of crosslinking within the microspheres beyond the gel point. The mean diameter of unswollen microspheres was determined solely by the first factor. Swelling of microspheres was determined solely by the second factor. The mean diameter of swollen microspheres was thus dependent on both factors. The microsphere sizes were polydisperse, which likely reflected the distribution of sizes of phase domains generated during coarsening. Using the principles outlined here, the size and density of the 100% PEG microspheres may be engineered with high precision for a variety of end applications.

Supplementary Material

Refer to Web version on PubMed Central for supplementary material.

Acknowledgments

The authors are grateful to Igor Efimov for use of the confocal microscope and funding from NIH R01HL085364 (DLE) and American Heart Association Predoctoral Fellowship 0715676Z (EAS). We thank Brandon George, Peter Nguyen, Casey Donahoe and Megan Flake for technical assistance.

References

1. Flodin, P. inventor Process for preparing hydrophilic copolymerization and product obtained thereby patent US. 3,208,994. 1965.
2. Nolan CM, Reyes CD, Debord JD, Garcia AJ, Lyon LA. Phase transition behavior, protein adsorption, and cell adhesion resistance of poly(ethylene glycol) cross-linked microgel particles. Biomacromolecules 2005;6:2032–2039. [PubMed: 16004442]
3. McGuigan AP, Sefton MV. Vascularized organoid engineered by modular assembly enables blood perfusion. Proceedings of the National Academy of Sciences 2006;103:11461–11466.
4. Yeh J, Ling Y, Karp JM, Gantz J, Chandawarkar A, Eng G, et al. Micromolding of shape-controlled, harvestable cell-laden hydrogels. Biomaterials 2006;27:5391–5398. [PubMed: 16828863]
5. Rivest C, Morrison DWG, Ni B, Rubin J, Yadav V, Mahdavi A, et al. Microscale hydrogels for medicine and biology: Synthesis, characteristics and applications. Journal of Mechanics of Materials and Structures 2007;2:1103–1119.
6. Kwok KK, Groves MJ, Burgess DJ. Production of 5–15-micron diameter alginate-polylysine microcapsules by an air-atomization technique. Pharm Res 1991;8:341–344. [PubMed: 2052521]

7. Um E, Lee D-S, Pyo H-B, Park J-K. Continuous generation of hydrogel beads and encapsulation of biological materials using a microfluidic droplet-merging channel. Microfluidics and Nanofluidics 2008;5:541–549.
8. Edman P, Ekman B, Sjoholm I. Immobilization of proteins in microspheres of biodegradable polyacryldextran. Journal of pharmaceutical sciences 1980;69:838–842. [PubMed: 6156234]
9. Franssen O, Hennink WE. A novel preparation method for polymeric microparticles without the use of organic solvents. International Journal of Pharmaceutics 1998;168:1–7.
10. Van Thienen TG, Demeester J, De Smedt SC. Screening poly(ethyleneglycol) micro-and nanogels for drug delivery purposes. International Journal of Pharmaceutics 2008;351:174–185. [PubMed: 18061378]
11. Van Tomme SR, Mens A, van Nostrum CF, Hennink WE. Macroscopic Hydrogels by Self-Assembly of Oligolactate-Grafted Dextran Microspheres. Biomacromolecules 2008;9:158–165. [PubMed: 18081253]
12. Jeon S, Lee J, Andrade J, DeGennes P. Protein Surface Interactions in the Presence of Polyethylene Oxide .1. Simplified Theory. Journal of Colloid and Interface Science 1991;142:149–158.
13. Bailey FE, Callard RW. Some properties of poly(ethylene oxide) in aqueous solution. J Appl Polym Sci 1959;1:56–62.
14. Bae YC, Lambert SM, Soane DS, Prausnitz JM. Cloud-Point Curves of Polymer-Solutions from Thermooptic Measurements. Macromolecules 1991;24:4403–4407.
15. Yen DR, Raghavan S, Merrill EW. Fractional precipitation of star poly(ethylene oxide). Macromolecules 1996;29:8977–8978.
16. Friedlander, SK. Smoke, Dust and Haze. New York: Wiley; 1977.
17. Ratke, L.; Voorhees, PW. Growth and Coarsening: Ostwald Ripening in Material Processing. Berlin: Springer-Verlag; 2002.
18. Friedlander SK, Wang CS. The self-preserving particle size distribution for coagulation by brownian motion. Journal of Colloid and Interface Science 1966;22:126–132.
19. Lifshitz IM, Slyozov VV. The Kinetics of Precipitation from Supersaturated Solid Solutions. J Phys Chem Solids 1961;19:35–50.
20. Crist B, Nesarikar AR. Coarsening in Polyethylene Copolymer Blends. Macromolecules 1995;28:890–896.
21. Wacker BK, Scott EA, Kaneda MM, Alford SK, Elbert DL. Delivery of sphingosine 1- phosphate from poly(ethylene glycol) hydrogels. Biomacromolecules 2006;7:1335–1343. [PubMed: 16602758]
22. Elbert DL, Hubbell JA. Conjugate Addition Reactions Combined with Free-radical Cross-linking for the Design of Materials for Tissue Engineering. Biomacromolecules 2001;2:430–441. [PubMed: 11749203]
23. Crist B. On "pinning" domain growth in two-phase polymer liquids. Macromolecules 1996;29:7276–7279.
24. Termonia Y. Molecular modeling of structure development upon quenching of a polymer solution. Macromolecules 1997;30:5367–5371.
25. Vemury S, Pratsinis SE. Self-preserving size distributions of agglomerates. Journal of Aerosol Science 1995;26:175–185.
26. Friedman M, Wall JS. Additive Linear Free-Energy Relationships in Reaction Kinetics of Amino Groups with alpha, beta-Unsaturated Compounds. J Org Chem 1966;31:2888–2894.
27. Lauger J, Lay R, Gronski W. The percolation-to-cluster transition during spinodal decomposition of an off-critical polymer mixture. Observation by light scattering and optical microscopy. The Journal of Chemical Physics 1994;101:7181–7184.
28. Siggia ED. Late stages of spinodal decomposition in binary mixtures. Physical Review A 1979;20:595.
29. Flory PJ. Statistical mechanics of swelling of network structures. J Chem Phys 1950;18:108–111.
30. Kruyt, HR. Colloid Science. Vol. Vol. I. Amsterdam: Elsevier; 1949.

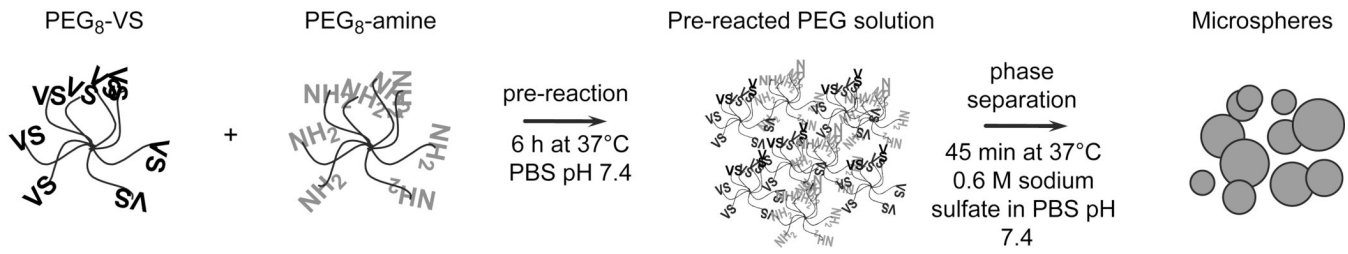

Figure 1.

Microsphere production from eight-arm PEG-vinylsulfone (PEG_8-VS) reacted with eight-arm PEG-amine (PEG_8-amine). The Michael-type reaction was followed by dynamic light scattering (DLS) to detect the formation of PEG oligomers/microgels during crosslinking prior to phase separation ('pre-reaction'). At a certain mean microgel diameter, the pre-reacted solution was diluted in PBS + 0.6 M sodium sulfate and then heated above the cloud point to produce microspheres.

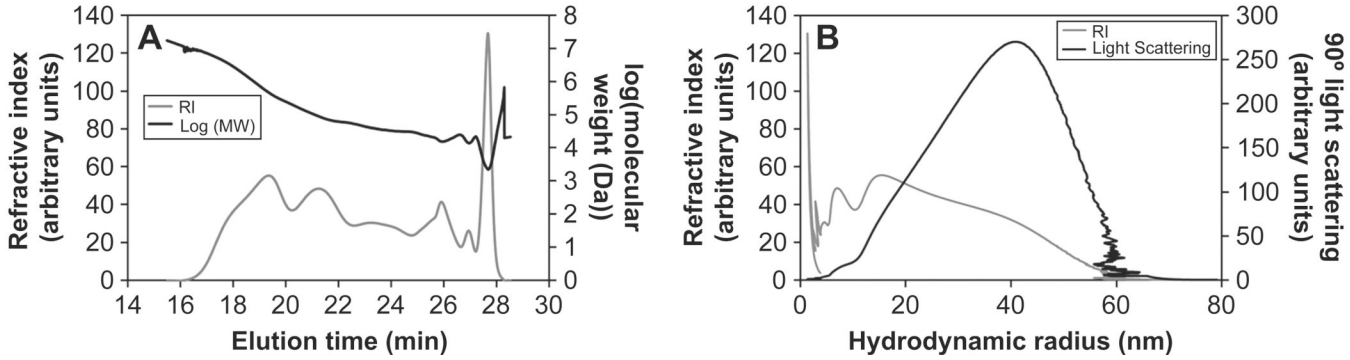

Figure 2.

Gel permeation chromatography of PEG_8-VS and PEG_8-amine pre-reacted to $d_{PCS} \cong 150$ nm. The reaction was halted by capping remaining vinyl sulfone groups with 2-mercaptoethanol. The absolute molecular weight was determined by detection of light scattering and refractive index. A) Molecular weight (black) and refractive index (gray) of eluted polymers. The peak at 27.6 min was confirmed to be monomeric PEG_8-VS in a separate run. B) Intensity of right angle light scattering (black) plotted against hydrodynamic radius. This should correspond well to the signal recorded by DLS of the pre-reacted samples. Refractive index (gray) is shown for comparison.

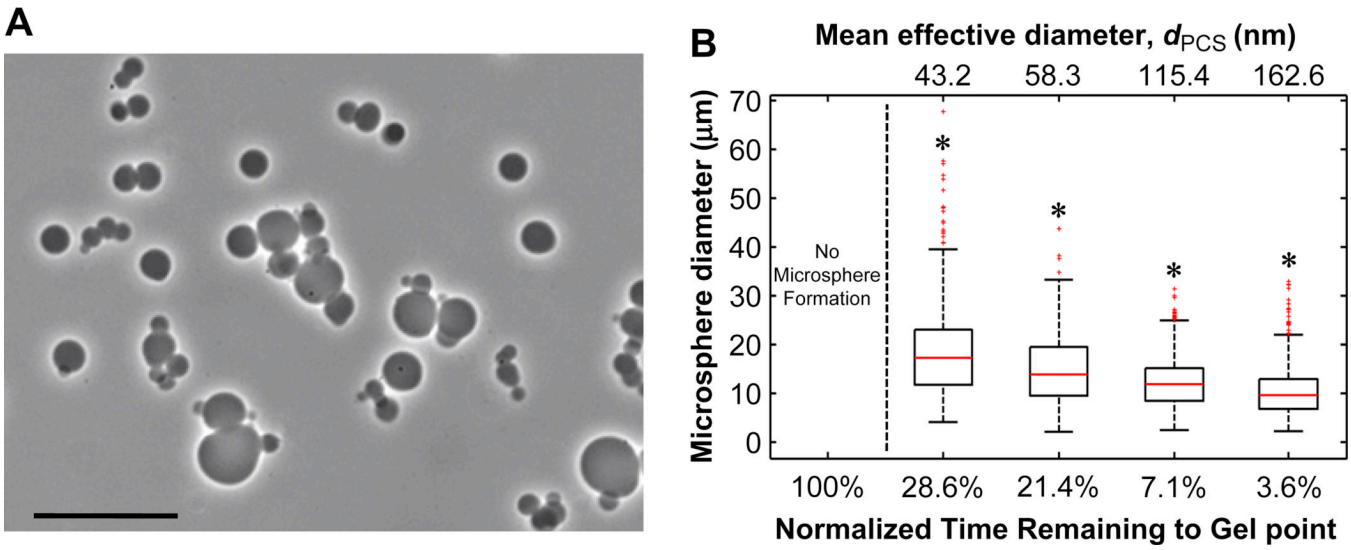

Figure 3.

Pre-reaction of PEG below the cloud point promoted microsphere formation. A) Phase-contrast photomicrograph at 20× magnification of PEG_8-VS/PEG_8-amine microspheres following buffer exchange into PBS. Scale bar represents 50 μm. B) PEG_8-VS and PEG_8-amine were pre-reacted below the cloud point to various degrees. Solutions were diluted to 2% (w/v) PEG in PBS + 0.6 M sodium sulfate, incubated for 45 min at 37°C and buffer exchanged into PBS. Under these conditions, stable microspheres were only formed using pre-reacted PEG. Increased pre-reaction (less time to gel point or larger d_{PCS} values) significantly decreased the sizes of mean microsphere diameters. Data represent n = 500 microspheres. * $p < 0.05$ versus all other conditions.

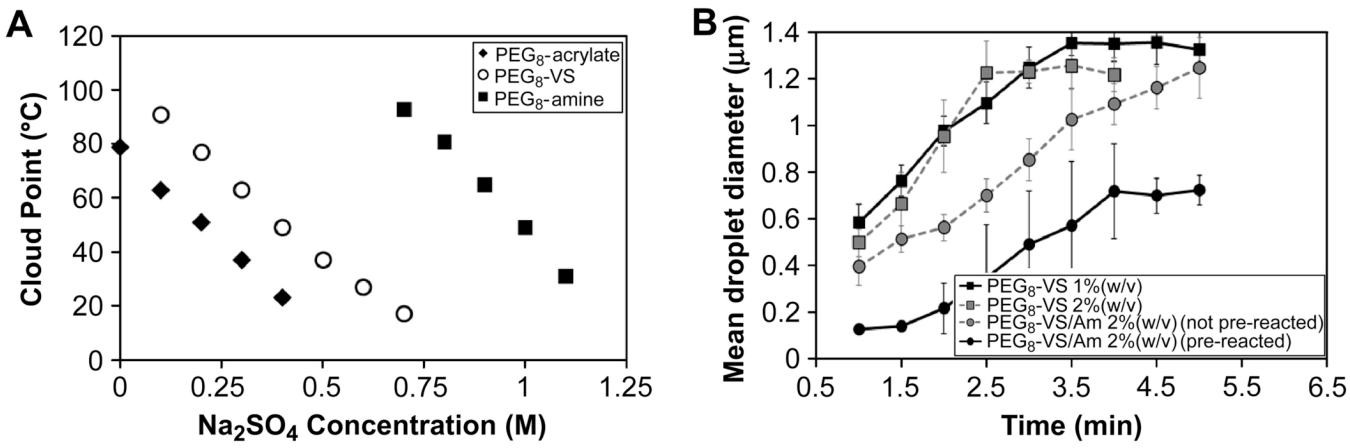

Figure 4.

A) Cloud points of 2% (w/v) PEG_8-VS, PEG_8-amine (PEG_8-Am) and PEG_8-acrylate (PEG_8-Ac) in PBS + sodium sulfate at pH 7.4. Data represent $n = 3$ and standard deviations were ≤ 1°C for all points. B) DLS of PEG solutions above their cloud points demonstrated that mean effective droplet diameters (d_{PCS} values) increased linearly with time during early stages of coarsening, as expected for the early stage of phase separation. Later, an apparent plateau in coarsening was observed, possibly corresponding to a percolation-to-cluster transition. Mixing PEG_8-VS with PEG_8-Am just prior to phase separation had little effect on the early stage of coarsening. Pre-reaction of these components to $d_{PCS} \cong 100$ nm delayed phase separation and led to a plateau at a much lower mean diameter. Data represent three independent samples averaged over 10 runs.

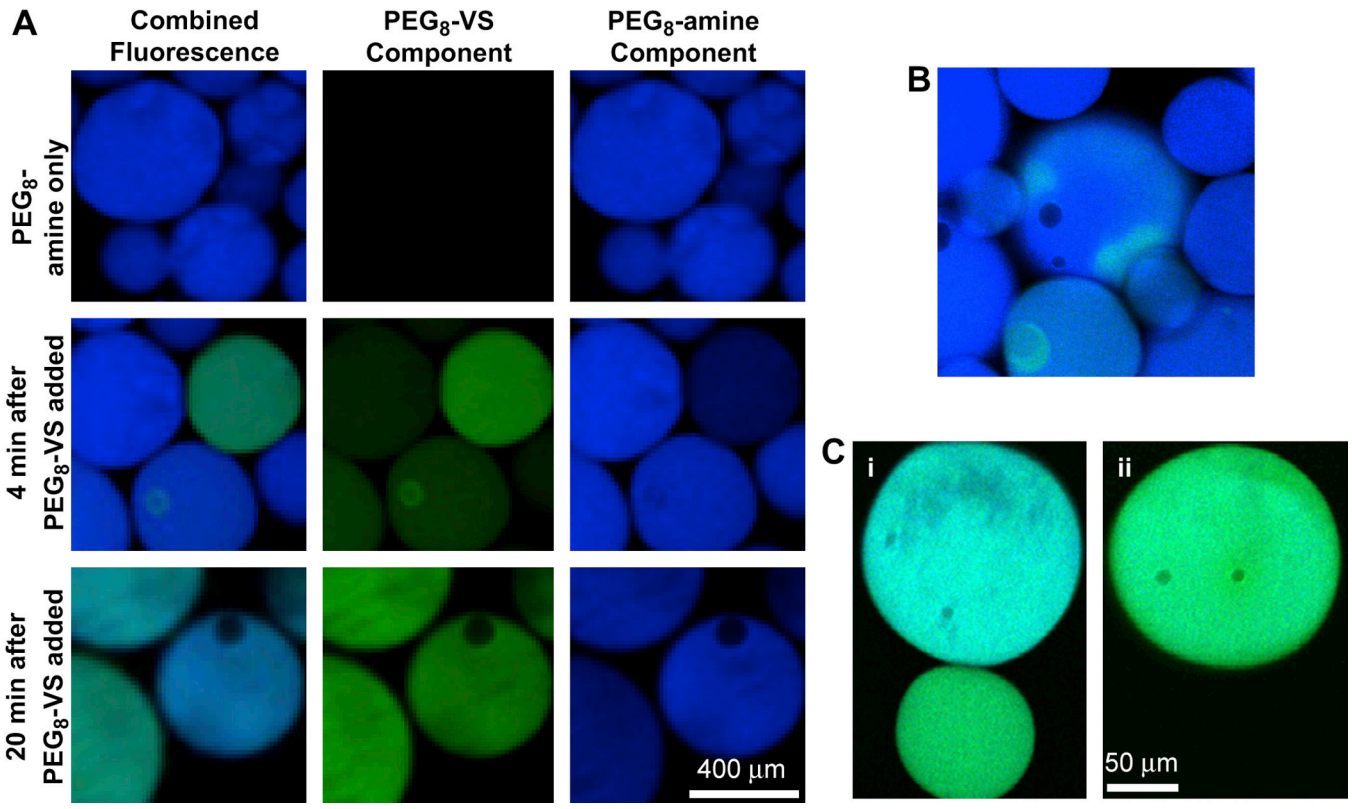

Figure 5.

The formation of PEG_8-VS/PEG_8-amine microspheres was observed by confocal microscopy using fluorescently labeled PEG derivatives. A) PEG_8-VS (green) and PEG_8-amine (blue) were separately added to PBS + 1.2 M sodium sulfate to cause phase separation at room temperature. The phase separated solutions were then mixed. Mass transfer occurred between the droplets without coalescence, indicating that Ostwald ripening may contribute to coarsening. B) Mass transfer was also directly observed under the same conditions between adjacent PEG-rich droplets without coalescence. C) Using conditions more typical of microsphere formation, PEG-rich droplets are shown before (i) and after (ii) coalescence. PEG_8-VS (green) was pre-reacted with PEG_8-amine (blue) to $d_{PCS} \cong 100$ nm and then crosslinked above the cloud point for 15 min at 37°C in PBS + 0.6 M sodium sulfate.

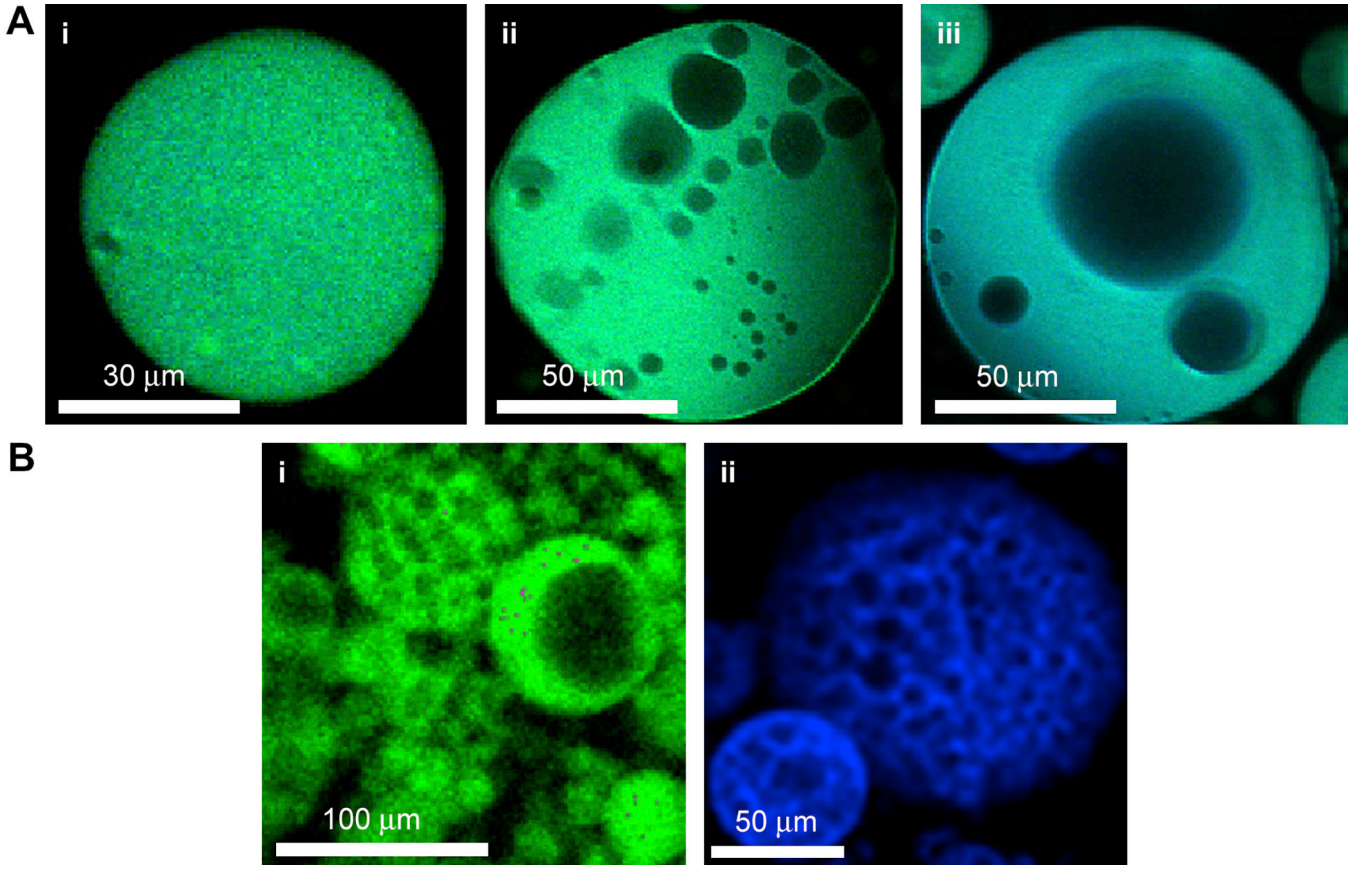

Figure 6.

Microspheres formed above the cloud point are porous. A) Development of water-rich droplets was observed within forming PEG_8-VS/PEG_8-amine microspheres by confocal microscopy. Fluorescently labeled PEG_8-VS (green) was mixed with PEG_8-amine (blue) in PBS + 0.6 M sodium sulfate and heated at 37°C for 15 min: (i–iii) progression of coarsening of water-rich domains within PEG-rich droplets over 15 min. B) To visualize the porous structure, larger microspheres were produced by pre-reacting all samples to $d_{PCS} \cong$ 100 nm and diluting in PBS + 0.8 M sodium sulfate, followed by reaction for 5 min above the cloud point at 25°C prior to further reaction as follows: (i) PEG_8-VS/PEG_8-amine (green), 37°C for 45 min (ii) PEG_8-acrylate/PEG_8-amine (blue), 95°C for 5 min.

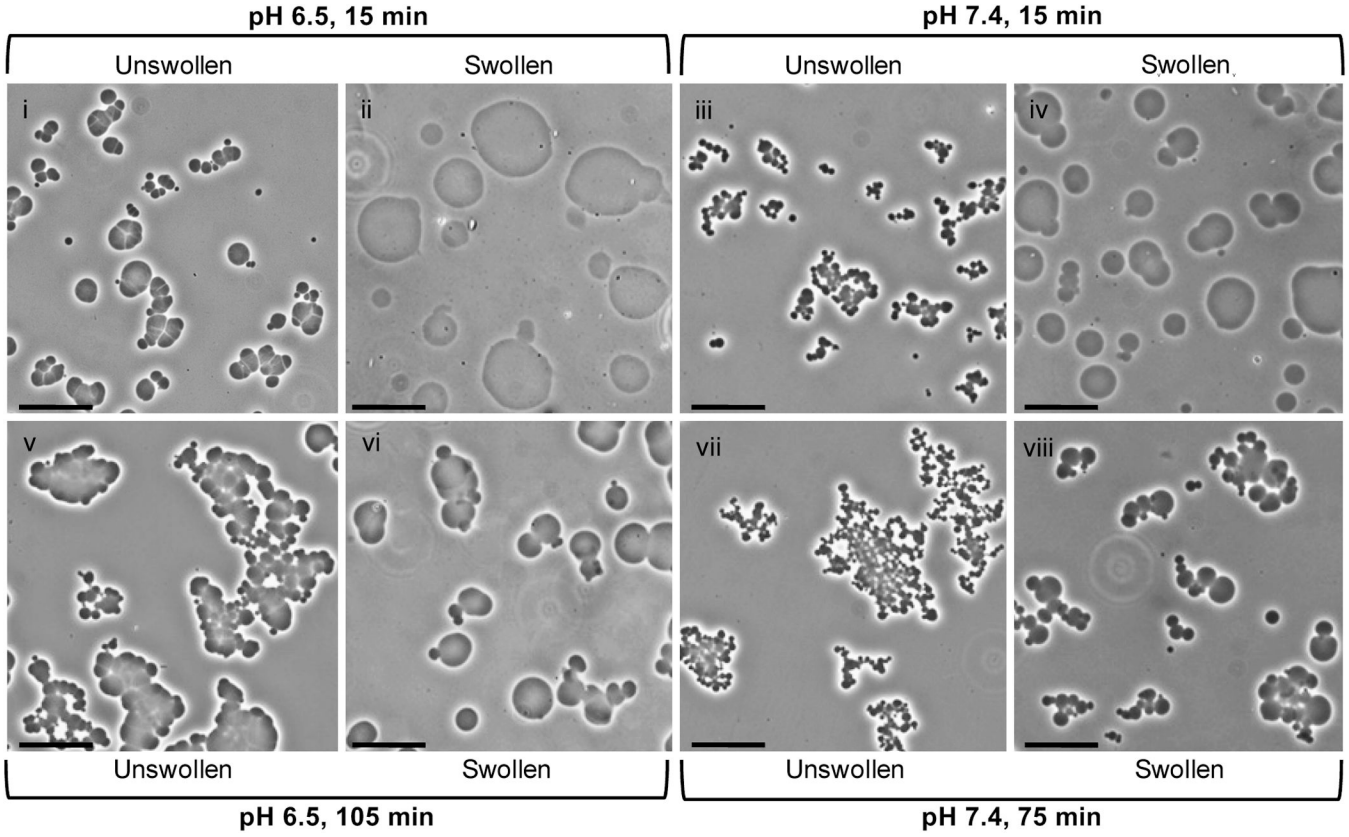

Figure 7.

Representative phase-contrast photomicrographs demonstrating swelling of PEG_8-VS/PEG_8-amine microspheres following buffer exchange into PBS. All microspheres were formed from pre-reacted solutions ($d_{PCS} \cong 100$ nm) diluted to 2% (w/v) in PBS + 0.6 M sodium sulfate and incubated at 37°C for: (i) 15 min at pH 6.5 without buffer exchange, (ii) 15 min at pH 6.5 with buffer exchange, (iii) 15 min at pH 7.4 without buffer exchange, (iv) 15 min at pH 7.4 with buffer exchange, (v) 105 min at pH 6.5 without buffer exchange, (vi) 105 min at pH 6.5 with buffer exchange, (vii) 75 min at pH 7.4 without buffer exchange, and (viii) 75 min at pH 7.4 with buffer exchange. Scale bars represent 25 μm.

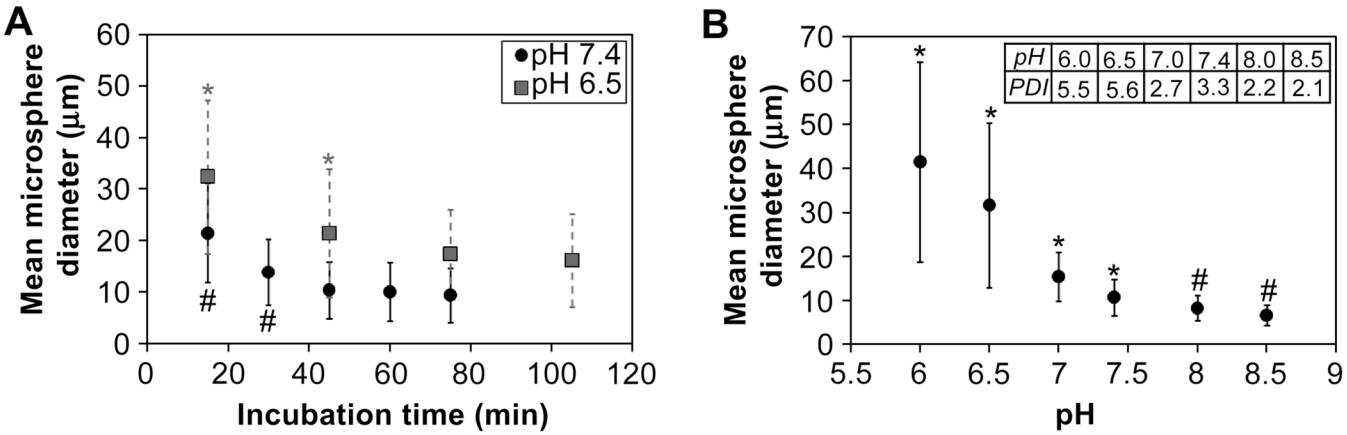

Figure 8.

Swollen microsphere sizes were affected by the reaction duration and pH. Unless otherwise stated, microspheres were formed from pre-reacted solutions of PEG_8-VS and PEG_8-amine ($d_{PCS} \cong 100$ nm) diluted to 2% (w/v) in PBS + 0.6 M sodium sulfate, incubated at 37°C for 45 min, and buffer exchanged into PBS. A) Microsphere diameters decreased with increasing incubation time above the cloud point, with pH 6.5 microspheres approaching but not matching pH 7.4 sizes even at extended times. For pH 6.5 reactions, PEG solutions were pre-reacted to $d_{PCS} \cong 150$ nm to allow multiple observations prior to microsphere aggregation/bulk gel formation. Data represent $n = 500$ microspheres at each timepoint. * $p < 0.05$ versus the 105 min timepoint for pH 6.5 and $^{\#}$ $p < 0.05$ versus the 75 min timepoint for pH 7.4. No significant changes in size were observed after 75 min at pH 6.5 or after 45 min at pH 7.4. B) Microsphere diameters and polydispersity indices (PDIs) were observed to decrease with increasing pH. Data represent $n = 500$ microspheres at each pH. * $p < 0.05$ versus all other pHs and $^{\#}$ $p < 0.05$ versus pH 6.0 –7.4.

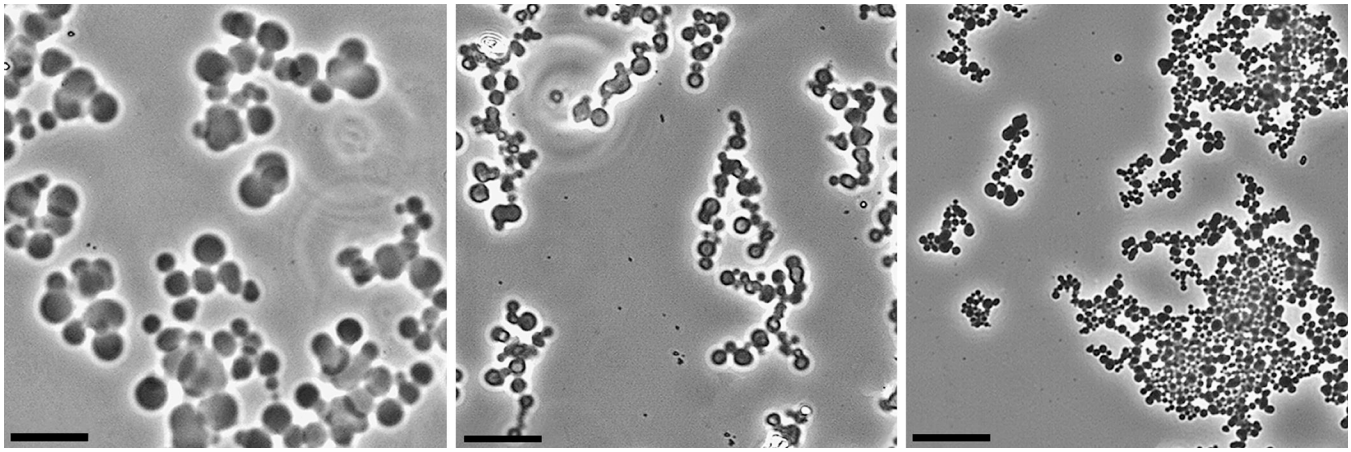

Figure 9.
Temperature effect on swollen microsphere sizes. Phase-contrast photomicrographs of microspheres produced from pre-reacted solutions of PEG_8-VS and PEG_8-amine ($d_{PCS} \cong 100$ nm) diluted to 2% (w/v) in PBS + 0.6 M sodium sulfate and incubated at pH 7.4 for: (i) 45 min at 37°C (ii) 10 min at 65°C (iii) 5 min at 95°C. Scale bars represent 25 μm.

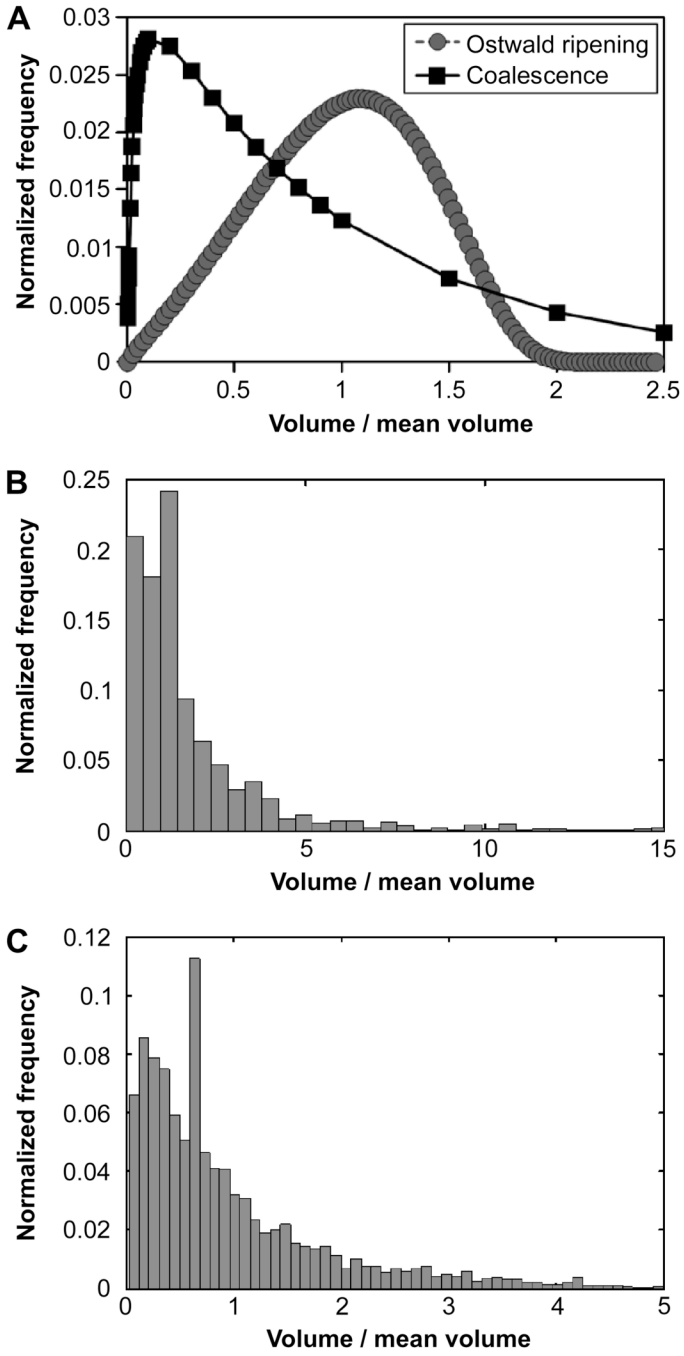

Figure 10.

Distributions of formed microspheres were similar to those expected for coalescence. A) Theoretical size distributions expected to result from Ostwald ripening or coalescence. B and C) Observed distributions of PEG_8-VS/PEG_8-amine microspheres formed from pre-reacted solutions of PEG_8-VS and PEG_8-amine ($d_{PCS} \cong$ 100 nm) diluted to 2% (w/v) in PBS + 0.6 M sodium sulfate and incubated at 37°C for 45 min at: (B) 7.4 (C) 8.5. Histograms were constructed using 100 bins for 500 randomly selected microspheres for each pH.

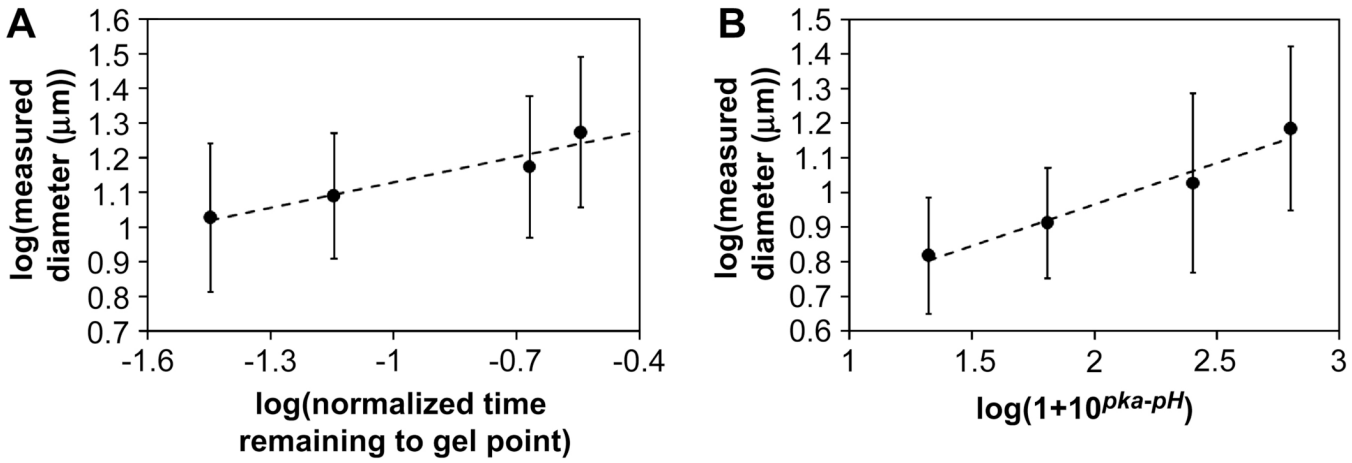

Figure 11.

Microsphere size as a function of characteristic time to the gel point revealed similar growth laws during coarsening. Power law plots of mean microsphere diameter versus: (A) normalized time remaining to the gel point based on the degree of pre-reaction using the data in Fig. 2B. (B) the pH-dependent amine reactivity using the data from Fig. 8B. Linear regression yielded slopes equal to 0.24 for both plots. The expected value for coarsening by Ostwald ripening and/or coalescence is 1/3, corresponding to an $R \propto time^{1/3}$ growth law, where R is the mean radius of the phase-separated domains. Standard deviations were calculated by propagation of error.

Table 1

Swelling ratios of microspheres in Fig 7. Q was the ratio of the unswollen mean volume to the swollen mean volume, with volumes calculated from mean diameters.

	pH 6.5		pH 7.4	
Incubation time (min)	15	105	15	75
Mean unswollen diameter (mm)	8.78±3.83	8.37±3.65	5.51±1.91	4.90±1.66
Mean swollen diameter (mm)	32.41±14.92	16.10±8.99	21.44±9.65	9.36±5.29
Q (swelling ratio)	50.32	7.13	58.98	6.99

Note: differences in mean microsphere diameters were statistically significant except for unswollen microspheres at pH 6.5 (15 vs. 105 min) and pH 7.4 (15 vs. 75 min).